Pharm Res (2012) 29:1775–1786
DOI 10.1007/s11095-012-0700-1

RESEARCH PAPER

Inclusion Complex of Novel Curcumin Analogue CDF and β-Cyclodextrin (1:2) and Its Enhanced *In Vivo* Anticancer Activity Against Pancreatic Cancer

Prasad R. Dandawate • Alok Vyas • Aamir Ahmad • Sanjeev Banerjee • Jyoti Deshpande • K. Venkateswara Swamy • Abeda Jamadar • Anne Catherine Dumhe-Klaire • Subhash Padhye • Fazlul H. Sarkar

Received: 4 January 2012 / Accepted: 31 January 2012 / Published online: 10 February 2012

ABSTRACT

Purpose Several formulations have been proposed to improve the systemic delivery of novel cancer therapeutic compounds, including cyclodextrin derivatives. We aimed to synthesize and characterize of CDF-β-cyclodextrin inclusion complex (1:2) (CDFCD).

Methods The compound was characterized by Fourier transform infrared, differential scanning calorimetry, powder X-ray diffraction studies, H1 & C13 NMR studies and scanning electron microscopic analysis. Its activity was tested against multiple cancer cell lines, and *in vivo* bioavailability was checked.

Results CDF-β-cyclodextrin was found to lower IC_{50} value by half when tested against multiple cancer cell lines. It preferentially accumulated in the pancreas, where levels of CDF-β-cyclodextrin in mice were 10 times higher than in serum, following intravenous administration of an aqueous CDF-β-cyclodextrin preparation.

Conclusions Novel curcumin analog CDF preferentially accumulates in the pancreas, leading to its potent anticancer activity against pancreatic cancer cells. Synthesis of such CDF-β-cyclodextrin self-assembly is an effective strategy to enhance its bioavailability and tissue distribution, warranting further evaluation for CDF delivery in clinical settings for treatment of human malignancies.

KEY WORDS CDF· curcumin analog · CDF-β-Cyclodextrin · pancreatic cancer

INTRODUCTION

Curcumin (Diferuloylmethane) is the yellow colored spice constituent derived from the plant *Curcuma longa* (Linn) grown in tropical Southeast Asia and is one of the most investigated phytochemical for chemopreventive and therapeutic uses (1). The compound has been shown to inhibit the growth and proliferation of a variety of tumor cells (2). However, poor bioavailability and rapid metabolism of Curcumin has limited its application in the clinic (3). Recently, we have developed a novel synthetic analogue of Curcumin, viz. 3, 4-difluorobenzo curcumin (named as Difluorinatedcurcumin, CDF) which has shown greater bioavailability in pancreatic tissues, enhanced inhibition of cancer cell growth, DNA-binding activity of NF-κB, Akt, COX-2, production of PGE_2 and VEGF, re-expressed miR-200 and down-regulated miR-21 in pancreatic cancer cells (4-6). More recent data from our laboratory has shown a

Electronic supplementary material The online version of this article (doi:10.1007/s11095-012-0700-1) contains supplementary material, which is available to authorized users.

P. R. Dandawate • A. Vyas • S. Padhye
ISTRA, Department of Chemistry, MCE Society's Abeda Inamdar Senior College of Arts, Science and Commerce
Pune 411001, India

A. Ahmad • S. Banerjee • S. Padhye (✉) • F. H. Sarkar (✉)
Department of Pathology, Barbara Ann Karmanos Cancer Center
Wayne State University School of Medicine
740 HWCRC,
Detroit, Michigan 48201, USA
e-mail: sbpadhye@hotmail.com
e-mail: fsarkar@med.wayne.edu

A. Vyas • J. Deshpande • K. V. Swamy
Dr. D. Y. Patil Biotechnology and Bioinformatics Institute
Tathawade, Pune 411044, India

A. Jamadar • A. C. Dumhe-Klaire
Department of Chemistry, University of York, Heslington
York YO10 5DD, UK

very potent action of CDF against cancer stem cells (CSCs), which was mediated through deregulation of multiple miRNAs, induction of PTEN and attenuation of histone methyltransferase EZH2 (7,8). CDF was also found to inhibit signal transduction in the AR/TMPRSS2-ERG/Wnt signaling network, leading to the inactivation of Wnt signaling consistent with inhibition of prostate cancer cell invasion (9). Interestingly, down-regulation of miR-21 expression upon CDF treatment resulted in the induction of PTEN (6,7). Our investigations have also suggested that CDF together with the conventional chemotherapeutics could be an effective treatment strategy for preventing the emergence of chemo-resistant colon cancer cells by eliminating colon CSCs (10). These findings suggest that CDF could be a useful option for the prevention of tumor recurrence and better treatment outcome for human malignancies especially for pancreas cancer for which newer therapeutic option is urgently needed.

Several investigations have dealt with formulation and drug delivery aspects of curcumin for improving its bioavailability and water solubility, including nanoparticles (11), nanocapsules (12), liposomes (13) and various derivatives of cyclodextrins (CD) (14–16). Among these, cyclodextrin formulations were shown to enhance water solubility of curcumin by about 100 times with improved anti-inflammatory and anti-angiogenic activity (17). Recent research has also indicated that β-cyclodextrin-curcumin inclusion complex is more effective in inducing apoptosis in leukemic cells along with enhanced inhibitory activity of TNF-induced activation of the inflammatory transcription factor NF-κB and in suppressing gene products regulated by it (18). The compound was also shown to have greater cellular uptake and longer half-life in the KBM-5 cells. Similar trend has also been reported by Chauhan and co-workers suggesting that β-cyclodextrin self-assembly with curcumin-like molecules may be a good choice for enhanced delivery and improved therapeutic efficacy towards cancer cells, compared to free curcumin (19). Here we describe for the first time the detailed synthesis, characterization and anticancer activity of 1:2 CDF-cyclodextrin conjugate (CDFCD). We also report on the bioavailability of this novel conjugate, with specific focus on its accumulation in the pancreas, the tissue where CDF was documented to be accumulated in our earlier reports.

MATERIALS AND METHODS

Phase Solubility Analysis

CDF was synthesized as reported earlier (4). Phase solubility study was carried out by the method reported by Higuchi and Connors (20). Different concentrations of β-cyclodextrin solutions such as 0, 2, 6, 8, 10, and 20 mM were prepared in distilled water and filled in screw capped bottles. Excess CDF was added to these solutions to attain saturation. Each bottle was capped and shaken for 72 h in a constant temperature water bath at 30±2°C. Following equilibrium, these solutions were filtered using 0.45-μm nylon disk filter, diluted, and assayed for the total dissolved CDF content by UV analysis at 365 nm. Each sample was determined in triplicate and the samples were protected from light. The phase solubility diagram was constructed by plotting concentrations of dissolved CDF against cyclodextrin concentration.

Preparation of Inclusion Complexes and Solubility Studies

Kneading method was used for the preparation of cyclodextrin inclusion complexes of CDF wherein the constituents in 2:1 molar ratio were mixed in a mortar for 1 h with alcohol and distilled water mixture to get slurry-like consistency. The paste was dried in a hot air oven at a temperature of 45°C for 24 h. Dried complex was pulverized into fine powder and sifted with sieve # 80. Excess of CDF and CDFCD (1:2) complex were dispersed in 25 ml of distilled water in screw-capped bottles to get a supersaturated solution. These bottles were shaken continuously for 2 h at ambient temperature until equilibrium was attained. Supersaturated solution was filtered through a 0.22-μm nylon filter and further diluted with methanol and absorbance was measured at 365 nm.

Infra-red / Differential Scanning Calorimetric / X-ray Diffraction Studies

Infra-red spectra of CDF, β-cyclodextrin and CDFCD were measured on Shimadzu Fourier Transform Infrared (FTIR)-8700 spectrophotometer by potassium bromide disk method. Samples were mixed with dry powdered potassium bromide and compressed into transparent disk under high pressure and scanned over 4,000–400 cm^{-1}region. Differential Scanning Calorimetric (DSC) studies of CDF, β-cyclodextrin and CDFCD were performed using Mettler DSC Toldeo (Switzerland) instrument. Samples were weighed (5.00–8.00±0.5 mg) and placed in sealed aluminum pans. The coolant was liquid nitrogen. The samples were scanned at 10°C/min from 20°C to 300°C and thermograms were recorded. X-ray diffraction patterns of CDF, β-cyclodextrin and CDFCD were determined using a diffractometer (Bruker, AXS D-8 Advance) equipped with a rotating target X-ray tube and a wide-angle goniometer. The X-ray source was Kα radiation from a copper target with graphite monochromater. The X-ray tube was operated at a potential of 50 kV and a current

of 150 mA. The range (2θ) of scans was from 5° to 50° at a speed of 2° per minute at increments of 0.1°.

Scanning Electron Microscope / Nuclear Magnetic Resonance Studies

Surface morphology of CDF, β-cyclodextrin and CDFCD were examined by Scanning Electron Microscope (SEM; Jeol JST-6360A). Samples were dispersed onto carbon tabs (double-adhesive carbon coated tape) adhered to aluminum stubs. These sample stubs were coated with a thin layer (30 Å) of gold by employing Jeol JFC-1600 auto fine coater. Samples were subsequently examined by SEM and photographed under various magnifications with direct data capture of the images onto a computer. All NMR spectra were recorded in DMSO-d6 solvent using Jeol ECS 400 (^{1}H NMR 400 MHz, ^{13} C 100.6 MHz) spectrophotometer. Chemical shifts (δ) as given in terms of parts per million (ppm) are referenced to the residual solvent DMSO, ^{1}H NMR- 2.50 ppm, ^{13} C NMR-39.52 ppm. The spectra were processed using Bruker's TOPSPIN software. The following parameters were used during the NMR experiments: number of scans, 64; relaxation delay, 1.0 s; and pulse degree, 25°C.

Cyclic Voltammetric Studies

Electrochemical studies for the CDF and CDFCD were carried out in DMSO solvent using Bioanalytical System Epsilon (BASi) electrochemical analyzer. All experiments were carried out at room temperature by using DMSO as solvent and in presence of Tetrabutyl- ammonium perchlorate (TBAP) as supporting electrode. The three-electrode system consisted of Platinum disc as the working electrode, Ag/AgCl as the Reference electrode and Platinum wire as the auxiliary electrode. Nitrogen gas was purged in the solution for 30 min before starting the measurements. Cyclic voltammetry was run in the potential range of +800 and -1600 mV, current at 100 μA, quiet time of 2 s. and the scan-rate of100 mV/s. The software program provided by BASi was used to plot the graph of current (μA) Vs potential (mV).

Molecular Docking Studies

3D molecular structure of CUR and CDF were designed by CORINA software (21) by providing smiles from Molinspiration (www.molinspiration.com). Ligands were energy minimized to obtain stable conformation of bonds and angles in PRODRG server. 3D structure of beta-CD was obtained from the protein complex of alpha-amylase (pdb id: 1jl8.pdb) available from the protein data bank. The CD was then extracted and added polar hydrogen to full fill the valency along with energy minimization. CDF was considered as ligand and CD as a receptor for docking studies. Docking was performed to obtain a population of possible conformations and orientations for the ligands at the binding site. All molecular docking studies were carried out in AutoDock Vina software by creating grid with 58X52X48 and grid centre defined as 36.822, 57.601 and 60.268 along with X, Y and Z-axis by implementing Lamarckian Genetic Algorithm (LGA). The best conformation was chosen with the lowest binding energy, after the docking search was completed. The interactions of CDF-CD conformers, including hydrogen bonds and the bond lengths were analyzed using PYMOL software.

For studying CDF-CD interaction in the 1:2 conjugate, the extracted CD from alpha- amylase was modeled in to 2CD in VMD software and energy minimized with PRODRG server. Stable conformations of CDF were docked in to 2CD with grid dimensions 72X86X46 along with grid center 24.772, 30.51 and 52.855 in the receptor cavity. All the docking studies were carried out with AutoDock Vina software and analyzed by PYMOL based on lowest binding energy and hydrogen bonds for stable conformations of ligands in 2CD.

Cell Culture

Pancreatic cancer cells BxPC-3 and breast cancer cells MDA-MB-231 were cultured in DMEM (Invitrogen, USA) supplemented with 10% FBS while prostate cancer cells PC3 were cultured in RPMI (Invitrogen, USA) supplemented with 10% FBS. All cells were cultured in a 5% CO_2-humidified atmosphere at 37°C. The cell lines have been tested and authenticated in core facility Applied Genomics Technology Center at Wayne State University. The method used for testing was short tandem repeat profiling using the PowerPlex 16 System from Promega.

Cell Growth Assay Using dye 3-[4, 5 Dimethylthiazol-2-yl]-2, 5 Diphenyltetrazolium Bromide (MTT Assay)

Cells were seeded in a 96-well culture plate. Each treatment had eight replicate wells and, moreover, each experiment was repeated at least three times. Test compounds were added to cells 24 h after seeding. At the end of treatment (72 h), MTT (0.5 mg/ml) was added and plates incubated at 37°C for 2 h, followed by replacement of media with DMSO at room temperature for 30 min. Ultra Multi-functional Micro plate Reader (TECAN) was used to record the absorbance.

Pharmacokinetics and Tissue Distribution Studies

Female ICR-SCID mice (8–10 weeks old) were purchased from Harlan Laboratories (Indianapolis, IN, USA). Mice

were housed and maintained under sterile conditions and were used in accordance with Animal Care and Use Guidelines of Wayne State University. Mice received standard Lab Diet 5021 (Purina Mills, Inc., Richmond, IN). Mice were randomly divided into two groups as detailed below. All mice were starved overnight prior to treatment. Compounds were dissolved in 1:1 ethanol / polysorbate 80 and further diluted 10 times with 5% glucose before administering intravenously (i.v.) to mice. Group-I: Mice were administered single dose of CDF (5.0 mg/mice). Blood and pancreas were harvested at indicated time points. ~200 μL blood was collected by cardiac puncture; collected blood samples were allowed to clot, centrifuged and serum was separated and stored at −80°C until analysis. Pancreas was harvested, washed with PBS, blotted dry, weighed, and stored at −80°C until analysis. Group-II: These mice were administered single dose of CDF-β-cyclodextrin (1:2) (12.5 mg/mice, equivalent to CDF content of 5.0 mg/mice). Blood and pancreas were harvested and processed, as described above. Levels in mouse serum and pancreas samples were determined using the validated high-performance liquid chromatography with tandem mass spectrometry (LC-MS/ MS) methods as described earlier (4).

RESULTS AND DISCUSSION

Synthesis and Characterization of CDF

Synthesis of CDF was carried out as described earlier (5). The FTIR spectra of the compound showed a broad peak at 3437–3315 cm^{-1} indicating presence of phenolic hydroxyl groups, while carbonyl (C = O) and C = C group frequencies were found in the region 1627–1568 cm^{-1}. The characteristic C-F stretching frequency was found around 1274 cm^{-1}. The electronic spectrum of CDF exhibited λ_{max} at 365.5 nm attributed to π-π* transition. H^1NMR studies showed the presence of two singlets at 3.793 ppm corresponding to two methoxy groups, while the two hydroxyl groups exhibited a singlet at 9.799 ppm. The appearance of a singlet at 8.008 ppm was attributed to presence of methylidine proton suggesting the formation of Knoevenagel condensate. Aromatic and olefin proton signals appear between 6.776 and 7.650 ppm (13H). The higher coupling constant of protons in the aromatic region (16.4 Hz) indicated the expected '*trans*' configuration. These results suggested that introduction of difluorobenzylidene moiety into curcumin motif induces asymmetry into CDF structure. This asymmetry has further been confirmed by C^{13}-NMR spectra where two different carbonyl signals were observed, one of them being in the same range of the Curcumin carbonyls at 187.6 ppm (22), while the second found in higher field region at 198.4 ppm due to additional resonance effects with the difluorobenzylidene moiety. Electrospray ionization-Mass spectroscopic results have indicated the molecular ion peak at 493.1473 and 491.1305 in positive and negative modes respectively.

CDF

M.P. (°C): 220, UV–Vis (DMSO): λ_{max} (nm): 365.5. IR (KBr disk), v, cm^{-1}: 3437–3315 (-OH) 2933–2841 (C-H. OCH_3), 1627–1568 (C = C, C = O), 1429 (olefinic C-H), 1274 (C-F), 1184–1163 (aromatic C–O), 1035–823 (C–O–C). H^1NMR (400 MHz, DMSO-D6) (δ, ppm) 3.793 (3H, OCH_3), 3.854 (3H, OCH_3), 6.776 (d, 1H, J=8.0 Hz), 6.854 (d, 1H, J=8.0 Hz), 6.919 (d, 1H, J=16.4 Hz), 7.111 (d, 1H, J=6.4 Hz, J=1.8 Hz), 7.295 (d, 2H, J=8.8 Hz, J=1.8 Hz), 7.392–7.432 (m, 3H), 7.482–7.650 (m, 4H), 8.008 (s, 1H, -CH methylidine), 9.799 (2H, OH). C^{13}NMR (100 MHz, DMSO-D6) (δ, ppm): 30.690, 55.76, 111.661, 112.315, 115.688, 118.149, 118.339, 118.555, 118.731, 123.736, 124.179, 125.405, 126.076, 127.150, 131.470, 137.033, 142.151, 144.928, 147.566, 148.019, 148.863, 148.987, 149.957, 150.240, 150.473, 151.360, 187.884, 197.051. ESIMS m/z: 493.1473 (M^+, ESI + ve) and 491.1305 (M^+-H, ESI-ve) in accordance with MF $C_{28}H_{22}F_2O_6$.

Phase Solubility Studies

The phase solubility diagram for the complex formation between CDF and β-Cyclodextrin is shown in Fig. 1a. This plot shows that aqueous solubility of the CDF increases linearly as a function of cyclodextrin concentration up to 16 mM followed by appearance of a plateau up to 20 mM indicating a negative deviation from linearity (23). The solubility diagram of CDF in the presence of β-Cyclodextrin can be classified as A_N type according to Higuchi and Connors (20) and may be attributed to the formation of soluble 1:2 CDF- β-Cyclodextrin inclusion complex.

Solubility Studies of CDF-β-Cyclodextrin Complexes

The water solubility of curcumin has been shown to be enhanced significantly after complexation with β-Cyclodextrin (Yadav *et al.*, 2009). In the present study, water solubility of CDF was found to be 0.014 mg/ml which increased to 0.032 and 0.089 mg/ml after interacting with β-Cyclodextrin in 1:1 and 1:2 stoichiometric proportions respectively (Supplementary Material Table SI). Since solubility and potency of CDF-cyclodextrin 1:2 conjugate was higher than CDF-cyclodextrin 1:1 complex, structural characterization as well as anticancer activity exploration is described in case of the former.

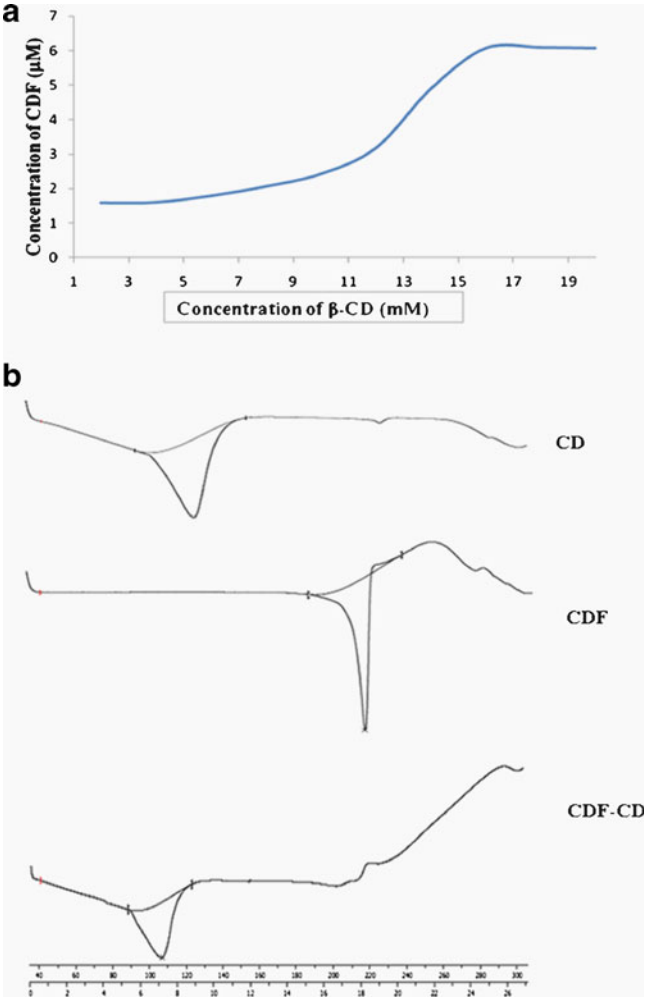

Fig. 1 (**a**) Phase solubility diagram CDF-β-cyclodextrin inclusion complex and (**b**) DSC spectra of cyclodextrin, CDF and CDF-cyclodextrin inclusion complex.

Infra-red Studies

Infra-red spectroscopic analysis was performed on CDF-cyclodextrin 1:2 conjugate to confirm the formation of CDF-β-cyclodextrin inclusion complex. The IR spectra and spectral assignments of β-cyclodextrin, CDF and CDFCD are shown in Supplementary Material Fig. S1 and Supplementary Material Table SII. The FTIR spectrum of CDF showed absorption bands at 3437–3315 cm^{-1} due to phenolic –OH stretches. Other sharp absorption bands were seen at 2933–2841 cm^{-1} (C-H. OCH_3), 1627–1568 cm^{-1} (C=C, C=O), 1429 cm^{-1} (olefinic C-H), 1274 cm^{-1} (C-F), 1184–1163 cm^{-1} (aromatic C–O) and 1035–823 cm^{-1} (C–O–C) respectively. FTIR spectrum of β-cyclodextrin alone exhibited intense peaks at 3377–3238 cm^{-1} and 2924 cm^{-1} due to O-H and C-H stretching vibrations as well as peaks at 1330, 1155–1078, 1030, 943 cm^{-1} indicating the presence of (C–C–H), (C–O–H), (H–C–H), (C–O), (C–C), (C–O–C), skeletal vibration involving α-1,4 linkage of glucose moiety and cyclodextrin rings (24).

In CDF-β-cyclodextrin 1:2 inclusion complex, all sharp peaks of β-cyclodextrin were observed along with few peaks of CDF. Observed peaks of CDF were found to exhibit lower intensity and reduced sharpness in CDFCD and β-cyclodextrin peaks were found to shift to lower or higher wave numbers. The intense peak of phenolic hydroxyl group was found to be shifted to 3373–3255 cm^{-1} and C-H stretching was shifted to 2928–2843 while C–C–H, C–O, C–C vibrations were observed at 858 cm^{-1} respectively. These results confirmed the intercalation of CDF in β-cyclodextrin and formation of CDF-β-cyclodextrin inclusion complex. The small differences in the FTIR peaks of β-cyclodextrin and CDF before and after inclusion complex formation suggests that there are no chemical bonds formed between CDF and β-cyclodextrin (25).

Differential Scanning Calorimetric Studies

Thermo-analytical studies are useful tools which provide information like physical state of drug present in various polymers, complexes or nano-particulate systems (26–29). It has been well-established that complexation of cyclodextrin with drug molecules leads to absence/shifting of endothermic peaks indicating a change in the crystal lattice, melting, boiling or sublimation points (30). Hence, such studies can be used for obtaining qualitative and quantitative information on the drug present in the cyclodextrin inclusion complexes. In present study, we have studied thermal properties of CDF, β-cyclodextrin and CDFCD by using Differential Scanning Calorimetric (DSC) method (Fig. 1b). β-cyclodextrin and CDF alone were found to exhibit endothermic peaks at 123.89°C (with onset at 102.6 and endset at 135.0°C) and 215.51°C (with onset at 208.6 and endset at 218.47°C) respectively, due to their melting temperatures. On other hand, CDFCD showed the diminished prominent melting peak of CDF at 215.51°C, while the β-cyclodextrin peak was shifted from 123.89 to 106.76°C (with onset at 89.41 and endset at 114.40°C). These results suggest that CDF molecules are probably included into the cavities of β-cyclodextrin indicating stronger solid state interactions between CDF and β-cyclodextrin. This type of behavior has earlier been reported in case of curcumin and β-cyclodextrin molecules (17,31).

X-Ray Diffraction Studies

X-Ray diffraction analysis has been used to analyze crystalline and amorphous nature of the drug and drug-polymer inclusion complexes. For analyzing CDF-β-cyclodextrin inclusion

complex, we conducted powder X-Ray Diffraction Studies. The powder X-Ray diffraction patterns of CDF, β-cyclodextrin and CDF-β-cyclodextrin inclusion complex are shown in Supplementary Material Fig. S2 and Supplementary Material Table SIII. The presence of numerous distinct peaks in PXRD of CDF at diffraction angles of (2θ) 10.7, 12.4, 16.1, 17.1, 19.4, 21.6, 23.2, 24.7, 25.0, and 25.6 are suggestive of the crystalline nature of CDF, while the β-cyclodextrin alone exhibits few crystalline peaks at 2θ 10.7,12.5, 17.1, 19.6, 20.8 and 22.8 respectively. The CDFCD conjugate showed low intensity peaks at 10.7, 12.4, 12.5, 16.1, 17.1, 19.4, 19.6, 20.8, 21.6, 22.8, 23.2, 24.7, 25.0 and 25.6. The percent intensity of peaks for CDFCD was found to be reduced as compared to CDF at 2θ values of 16.1 (51.75%), 17.1 (48.18%), 19.4 (34.09%), 21.6 (56.56%), 23.2 (51.79%), 24.7 (81.36%), 25.0 (57.55%), and 25.6 (66.93%) respectively suggesting that even CDF-β-cyclodextrin inclusion complex has not lost its crystalline nature. However, percent crystalline nature of CDF was lost significantly after complexation with β-cyclodextrin. Thus, the presence of some new peaks and loss in intensity of peaks of CDF and β-cyclodextrin suggest a change in crystal structure or modification of unit cell of β-cyclodextrin after formation of CDF-β-cyclodextrin inclusion complex. These observations indicate possible hydrogen bonding interactions between CDF and β-cyclodextrin.

Scanning Electron Microscope Studies

SEM studies were carried out to study bulk morphology of surface of CDF, β-cyclodextrin and CDFCD (Fig. 2) and SEM pictures revealed that β-cyclodextrin exhibits crystalline flakes- like structure, while CDF showed rod-like spherical-crystals. CDFCD was found to contain neither crystalline flakes nor needle like spherical-crystals, but showed irregular shaped micron-sized clumps or aggregates of CDF-β-cyclodextrin complexes. This change in morphology of CDFCD can be largely attributed to inclusion of CDF into β-cyclodextrin cavity suggesting a successful formation of CDF-β-cyclodextrin inclusion complex.

Cyclic Voltammetric Studies

Cyclic voltammetry (CV) has been used for studying the interaction between cyclodextrin and drug molecules (32,33). In present investigation we have also incorporated CV studies for analyzing inclusion complex of CDF with β-CD (Supplementary Material Fig. S3). The electrochemical profile of CDF showed existence of two reduction peaks at −1099 and −1411 mV respectively, whereas the oxidation peak appeared at 247 mV. The two reduction peaks may be attributed to the two carbonyl groups present in CDF molecule. The electrochemical behavior of CDFCD was found to be similar to CDF with significant shifting of peak positions towards positive potentials and decreased peak current (33,34). CDFCD was found to exhibit reduction peaks at −1103 mV and −1380 mV, while oxidation peak was seen at 294 mV. The anodic peak potential, $E_{pa,}$ was shifted in positive direction (+47 mV) and the anodic peak current, i_{ap}, was decreased from 3.27 μA to 2.10 μA in case of CDF. Similarly cathodic peak current i_{pc} was significantly decreased in case of CDFCD as compared to CDF. The decrease in current is attributed to slower diffusion coefficient from bulk layer to electrode surface of CDFCD inclusion complex than CDF. On the other hand, it was observed that the electrochemical oxidation of CDFCD was more difficult than that CDF due to entrapment of CDF into hydrophobic cavity of β-CD resulting in the shifting of anodic peak potential in positive direction (34). Thus, our electrochemical studies revealed hydrophobic interaction of CDF molecule in the cavity of β-CD, justifying the formation of CDFCD inclusion complex.

Nuclear Magnetic Resonance Spectroscopy

NMR spectroscopy is a powerful tool for the study of formation of inclusion complexes between cyclodextrin and a variety of guest molecules because the chemical and electronic environments of protons are affected during complexation and are reflected through changes in the δ values (35). Hence, the inclusion of CDF into the β-cyclodextrin cavity was studied by analyzing the changes observed in δ values of the protons in the complex in comparison with their values in free CDF and β-cyclodextrin molecules (Fig. 3; Supplementary Material Fig. S4, S5). The spectral assignments of β-cyclodextrin protons before (δ_{free}) and after formation of inclusion complex with CDF ($\delta_{complex}$) along with the Δδ values are indicated in Table I. Generally, it was observed that the resonances of the protons of β-cyclodextrin located within or near the cavity (H-3, 5, 6) exhibited large shifts in the mixture as compared to H-1, 2, 4 located on the exterior of β-cyclodextrin (36). In presence of CDF, protons of β-cyclodextrin undergo appreciable downfield shift (higher ppm) suggesting a successful interaction between CDF and β-cyclodextrin. These shifts could be the result of weak interactions (van der Waals forces) between CDF and β-cyclodextrin in the interior of the cavity. Shift to higher fields of the protons located within the drug and β-cyclodextrin cavity suggested that a hydrophobic interaction was predominant between the drug and the CD. These modifications in shifts of β-cyclodextrin protons also give evidence of the formation of partial or complete inclusion.

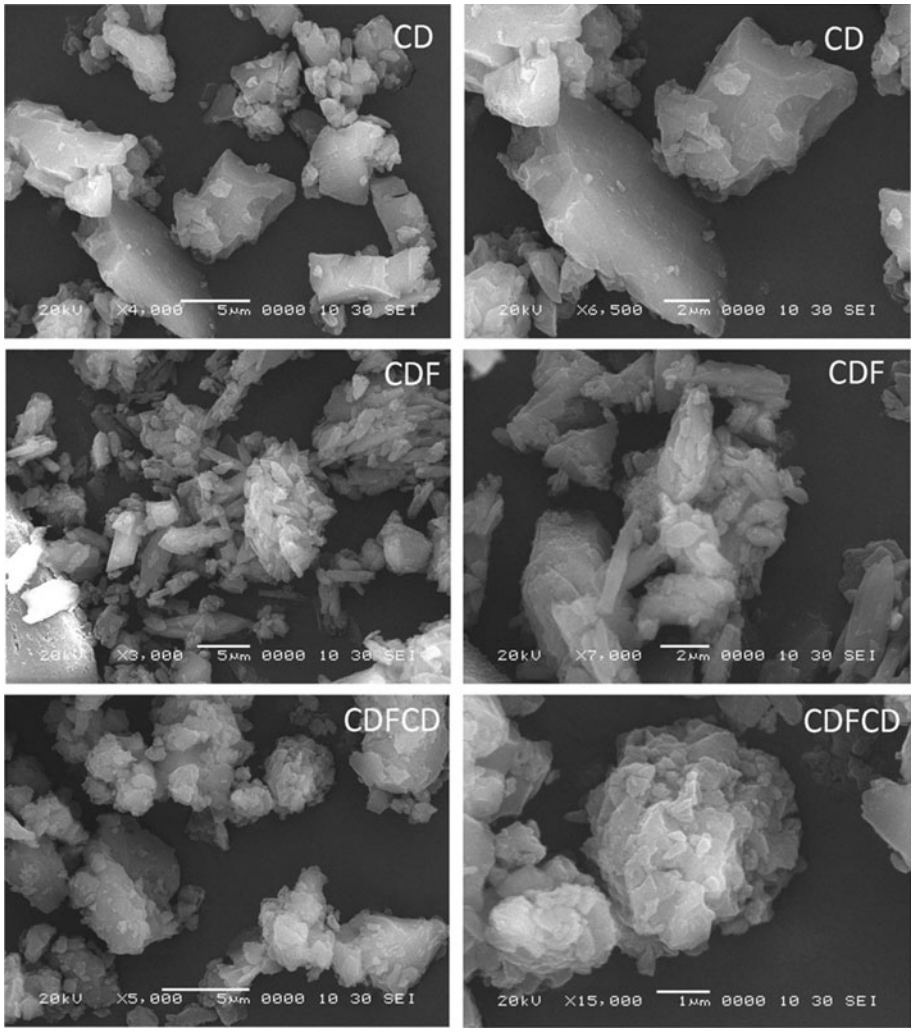

Fig. 2 Scanning electron microscopic images of cyclodextrin, CDF and CDF-cyclodextrin inclusion complex.

H^1-NMR analysis showed a shift of 0.016 and 0.008 ppm for the H-3 and H-5 protons of β-cyclodextrin, while a minor shift (0.006–0.009 ppm) was observed for other protons (H-1, H-2, H-4, H-6) respectively. Both the protons H-3 and H-5 are located in the interior of the β-cyclodextrin cavity with H-3 protons near the wide side of cavity and H-5 protons near the narrow side (37). The aromatic ring protons of CDF were found to appear in the range of 6.5–7.8 ppm, while all other protons were shifted up-field region (6.6–7.6 ppm) suggesting that these protons are involved in the complex formation with β-cyclodextrin. However, specific peaks of CDF between 6 and 8 ppm remain difficult to assign for their shifts, which is a typical for such inclusion complexes. Similar results have been noted in case of Curcumin-β-cyclodextrin inclusion complexes (19,38).

C^{13}-NMR study is one of the most useful methods in the analysis of the structure and molecular dynamics of cyclodextrin inclusion complexes in aqueous solution. C^{13}-NMR spectra of β-cyclodextrin, CDF and CDFCD shown in Supplementary Material Fig. S6 and Table I includes the spectral assignments of β-cyclodextrin carbons before (δ_{free}) and after formation of inclusion complex with CDF ($\delta_{complex}$) along with the $\Delta\delta$ values. All carbons of β-cyclodextrin exhibit downfield shift, while carbons on the aromatic rings of CDF show up-field shift indicating the formation of CDF-β-cyclodextrin inclusion complex. Thus, our H^1- and C^{13}-NMR spectroscopic results indicate a successful formation of CDF- β-cyclodextrin inclusion complex wherein the aromatic rings of CDF are included into β-cyclodextrin cavity from wider side.

Molecular Docking Studies

Molecular docking studies are found to be useful in predicting the orientation and interactions of drug molecules with β-cyclodextrin cavity (39). In the present study, we have

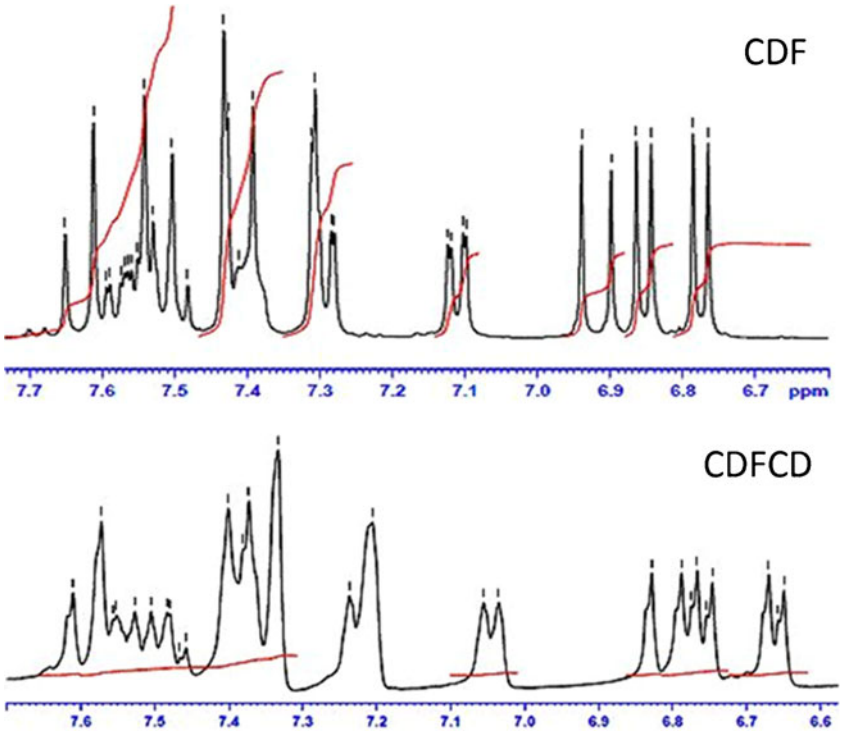

Fig. 3 Nuclear magnetic resonance spectra of cyclodextrin (CD) and CDF-β-cyclodextrin inclusion complex (selected region).

performed docking studies of CDF in β-cyclodextrin cavity. It was observed that CDF interacts with β-cyclodextrin in 1:2 ratios. We studied CDF interaction with β-cyclodextrin in 1:2 ratios leading to three possible conformers, which were referred as CDFCDc, CDFCDd and CDFCDe respectively (Fig. 4). The highest stable interaction observed in case of CDFCDc was found to involve aromatic ring containing difluoro and methoxy/hydroxyl groups with three hydrogen bonds (distances being 3.10, 3.50, 2.50 A^0 respectively) and binding energy of −6.50 Kcal/mol. The second stable interaction (CDFCDd) involves other aromatic ring containing

Table I H^1- and C^{13}-Nuclear Magnetic Resonance Assignments of β-Cyclodextrin in Free/Complex with CDF State, and Binding Energies of Interactions of CDF with β-Cyclodextrin, as Determined by Molecular Docking

H^1-NMR				C^{13}-NMR			
Proton	δ_{free}	$\delta_{complex}$	Δδ	Carbon	δ_{free}	$\delta_{complex}$	Δδ
H1	4.820	4.827	0.007	C1	60.024	60.051	0.027
H2	3.294	3.303	0.009	C2	81.629	81.653	0.024
H3	3.619	3.635	0.016	C3	102.045	102.069	0.024
H4	3.349	3.355	0.006	C4	72.140	72.168	0.028
H5	3.546	3.554	0.008	C5	73.156	73.196	0.040
H6	3.546	3.554	0.008	C6	72.497	72.538	0.041

H-1, 2, 3, 4, 5, 6a, b and C-1, 2, 3, 4, 5, 6 refer to the resonance of the protons and carbons of β-CD respectively.

Binding Energies of CDF - β-Cyclodextrin Interactions

Code	Ratio	No. of Polar Contacts Bonds	Bond Distance (A^0)	Binding Energy (Kcal/mol)
CDFCDc	1:2	3	3.10, 3.50, 2.50	−6.50
CDFCDd	1:2	1	2.30	−6.10
CDFCDe	1:2	–	–	−5.80

methoxy/hydroxyl and difluoro groups with one hydrogen bond (2.30 A^0) and binding energy of −6.10 Kcal/mol. The remaining CDFCDe conformer exhibits no hydrogen bonding interaction and lesser binding energy (−5.80 Kcal/mol) as compared to other conformers (Table I). These results are in accordance with our NMR studies confirming that the two aromatic rings of CDF are involved in the formation of stable interaction through hydrogen bonding with β-CD.

Anticancer Activity

The anticancer activity of CDF and CDF-β-cyclodextrin complexes (involving 1:1 and 1:2 molar ratios) were tested against pancreatic (BxPC-3), breast (MDA-MB-231) and prostate (PC3) cancer cells (Fig. 5). Though all compounds were found to inhibit the proliferation of the cancer cells tested, the 1:2 complex was found to be the most potent one. The IC-50 values of CDF against BxPC-3, MDA-MB-231 and PC3 cells were 350 nM, 325 nM and 260 nM whereas those of CDFCD 1:2 conjugate were 125 nM, 150 nM and 120 nM respectively.

Serum and Tissue Levels

Since CDFCD 1:2 conjugate was found to be more potent against the cancer cells examined, we used this formulation to test for its bioavailability. When administered to mice via i.v., the amount of CDFCD in the serum was determined to be ~110 ng/ml after 2 h and ~35 ng/ml after 4 h (Fig. 6a-b). Further, in view of our recent investigations on the efficacy of CDF in pancreatic cancer models (6–8) and our earlier report that CDF preferentially accumulates in pancreas (4), we focused on pancreas as the tissue of choice. We observed that CDFCD accumulated in pancreas of mice at concentrations of ~410 ng/ml and ~280 ng/ml after 2 h and 4 h respectively. These results indicate an enrichment of CDF formulation in pancreas where the levels were observed to be much higher than the circulating levels. We performed similar studies using parent compound CDF as well, and observed that the concentration of CDF was ~6 ng/ml at 2 h in serum and ~300 ng/g in pancreas (Fig. 6c-d). Our results indicate that the CDF-β-cyclodextrin 1:2 conjugate not only demonstrates increased anti-proliferative growth against cancer cells but is are associated with better bioavailability profile.

CONCLUSIONS

We have earlier reported synthesis of a novel Curcumin analog, CDF (5) with enhanced bioavailability and tissue distribution, compared to its parent compound curcumin. In an attempt to further improve its bioavailability and raise its clinical potential, we have synthesized and characterized β-cyclodextrin inclusion complexes of CDF. In particular, we found that the 1:2 CDF-β-cyclodextrin complex was much more potent than CDF alone or CDF:β-cyclodextrin 1:1 complex. IC_{50} values of this novel formulation against

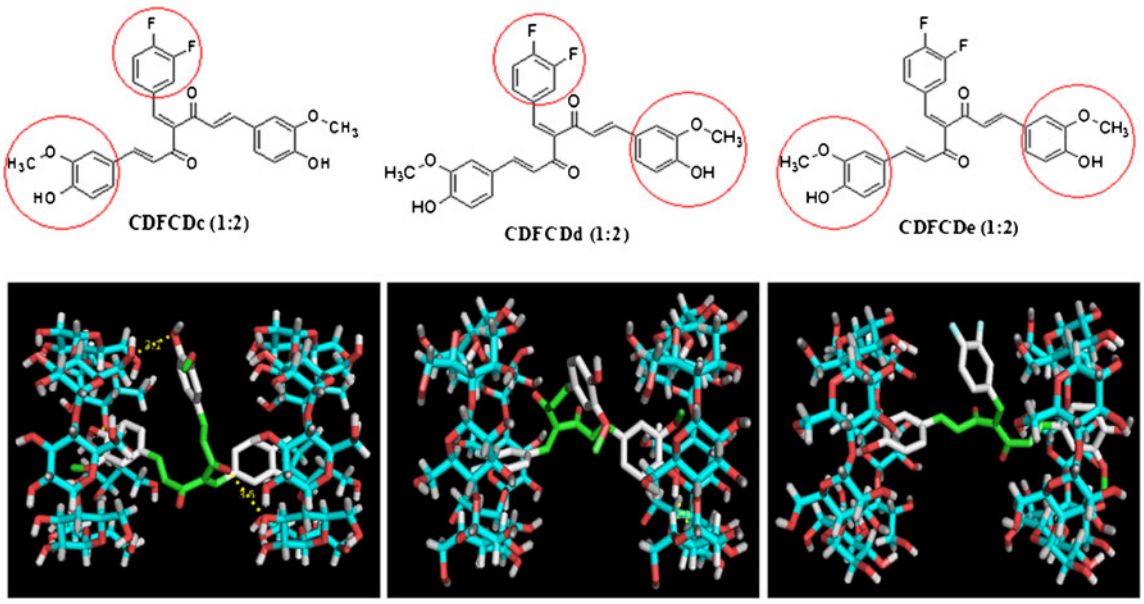

Fig. 4 Relative host–guest geometry corresponding to the minimum of the energy of the formations of CDF-β-cyclodextrin (1:2) by molecular docking.

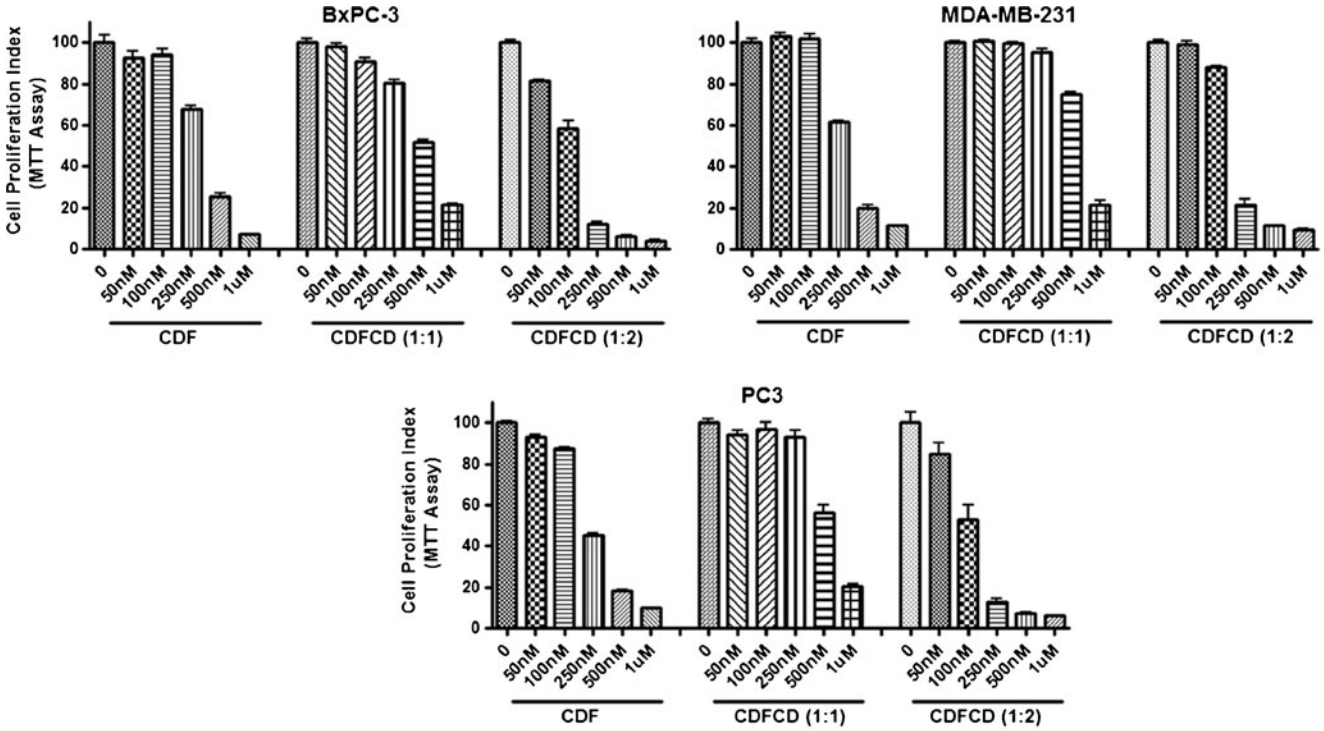

Fig. 5 Effect of CDF and CDF-β-cyclodextrins on cell growth of cancer cells, as determined by MTT assay.

multiple cancer cell lines, of pancreatic, breast and prostate origin, were more than halved and it was also found to be better bioavailable, as demonstrated by serum concentrations. Our recent work has established an anticancer action of CDF against pancreatic cancer cells, including an effective inhibition of pancreatic CSCs (7,8). Pancreatic cancer remains one of the worst cancer in terms of mortality rates (40) for which there are very limited therapeutic options. Increased accumulation of CDF:β-cyclodextrin 1:2 complex in the pancreas points to its potential use as a therapeutic agent against pancreatic cancer. Our earlier published results indicated preferential accumulation of CDF in the pancreas of mice where the levels of CDF were 10 times higher than those of curcumin (4). Here we observed that the levels of CDF:β-cyclodextrin 1:2 complex were about 10 times higher in pancreas than the serum. Our observations therefore support earlier results with regards to the accumulation of CDF in the pancreas but more importantly they point towards an enhanced bioavailability when complexed with β-cyclodextrin. Collectively, this study demonstrates that β-cyclodextrin inclusion is an effective strategy to enhance the systemic bioavailability and tissue distribution of CDF which raises the hope of further testing this compound in clinical settings for the targeted therapy of pancreatic cancer and other human malignancies.

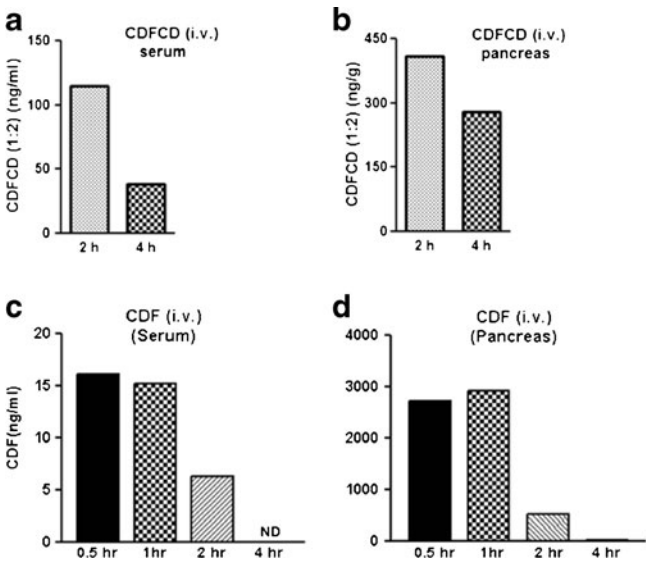

Fig. 6 Concentration *vs.* time profiling of CDF-β-cyclodextrin (1:2) in (**a**) mice serum and (**b**) pancreas, and of CDF in (**c**) mice serum and (**d**) pancreas following single i.v. administrations.

ACKNOWLEDGMENTS & DISCLOSURES

P.D. acknowledges CSIR, New Delhi, INDIA for providing Senior Research Fellowship. SP is thankful to Mr. P. A. Inamdar for his keen interest and encouragement. We acknowledge Department of Physics, University of Pune and R. C. Patel Institute of Pharmaceutical Education & Research, Shirpur, for providing SEM, PXRD and DSC facilities.

REFERENCES

1. Shishodia S, Sethi G, Aggarwal BB. Curcumin: getting back to the roots. Ann N Y Acad Sci. 2005;1056:206–17.
2. Ravindran J, Prasad S, Aggarwal BB. Curcumin and cancer cells: how many ways can curry kill tumor cells selectively? AAPS J. 2009;11:495–510.
3. Anand P, Kunnumakkara AB, Newman RA, Aggarwal BB. Bioavailability of curcumin: problems and promises. Mol Pharm. 2007;4:807–18.
4. Padhye S, Banerjee S, Chavan D, Pandye S, Swamy KV, Ali S, *et al.* Fluorocurcumins as cyclooxygenase-2 inhibitor: molecular docking, pharmacokinetics and tissue distribution in mice. Pharm Res. 2009;26:2438–45.
5. Padhye S, Yang H, Jamadar A, Cui QC, Chavan D, Dominiak K, *et al.* New difluoro Knoevenagel condensates of curcumin, their Schiff bases and copper complexes as proteasome inhibitors and apoptosis inducers in cancer cells. Pharm Res. 2009;26:1874–80.
6. Ali S, Ahmad A, Banerjee S, Padhye S, Dominiak K, Schaffert JM, *et al.* Gemcitabine sensitivity can be induced in pancreatic cancer cells through modulation of miR-200 and miR-21 expression by curcumin or its analogue CDF. Cancer Res. 2010;70:3606–17.
7. Bao B, Ali S, Kong D, Sarkar SH, Wang Z, Banerjee S, *et al.* Anti-tumor activity of a novel compound-CDF is mediated by regulating miR-21, miR-200, and PTEN in pancreatic cancer. PLoS One. 2011;6:e17850.
8. Bao B, Ali S, Banerjee S, Wang Z, Logna F, Azmi AS, *et al.* Curcumin analog CDF inhibits pancreatic tumor growth by switching on suppressor microRNAs and attenuating EZH2 expression. Cancer Res. 2012;72:335–45.
9. Li Y, Kong D, Wang Z, Ahmad A, Bao B, Padhye S, *et al.* Inactivation of AR/TMPRSS2-ERG/Wnt signaling networks attenuates the aggressive behavior of prostate cancer cells. Cancer Prev Res (Phila). 2011;4:1495–506.
10. Kanwar SS, Yu Y, Nautiyal J, Patel BB, Padhye S, Sarkar FH, *et al.* Difluorinated-curcumin (CDF): a novel curcumin analog is a potent inhibitor of colon cancer stem-like cells. Pharm Res. 2011;28:827–38.
11. Yallapu MM, Dobberpuhl MR, Maher DM, Jaggi M, Chauhan SC. Design of Curcumin loaded Cellulose Nanoparticles for Prostate Cancer. Curr Drug Metab. 2011.
12. Mazzarino L, Silva LF, Curta JC, Licinio MA, Costa A, Pacheco LK, *et al.* Curcumin-loaded lipid and polymeric nanocapsules stabilized by nonionic surfactants: an *in vitro* and *In vivo* antitumor activity on B16-F10 melanoma and macrophage uptake comparative study. J Biomed Nanotechnol. 2011;7:406–14.
13. Pandelidou M, Dimas K, Georgopoulos A, Hatziantoniou S, Demetzos C. Preparation and characterization of lyophilised egg PC liposomes incorporating curcumin and evaluation of its activity against colorectal cancer cell lines. J Nanosci Nanotechnol. 2011;11:1259–66.
14. Dhule SS, Penfornis P, Frazier T, Walker R, Feldman J, Tan G et al. Curcumin-loaded gamma-cyclodextrin liposomal nanoparticles as delivery vehicles for osteosarcoma. Nanomedicine. 2011.
15. Harada T, Pham DT, Leung MH, Ngo HT, Lincoln SF, Easton CJ, *et al.* Cooperative binding and stabilization of the medicinal pigment curcumin by diamide linked gamma-cyclodextrin dimers: a spectroscopic characterization. J Phys Chem B. 2011;115:1268–74.
16. Hegge AB, Schuller RB, Kristensen S, Tonnesen HH. *In vitro* release of curcumin from vehicles containing alginate and cyclodextrin. Studies of curcumin and curcuminoides. XXXIII. Pharmazie. 2008;63:585–92.
17. Yadav VR, Suresh S, Devi K, Yadav S. Effect of cyclodextrin complexation of curcumin on its solubility and antiangiogenic and anti-inflammatory activity in rat colitis model. AAPS PharmSciTech. 2009;10:752–62.
18. Yadav VR, Prasad S, Kannappan R, Ravindran J, Chaturvedi MM, Vaahtera L, *et al.* Cyclodextrin-complexed curcumin exhibits anti-inflammatory and antiproliferative activities superior to those of curcumin through higher cellular uptake. Biochem Pharmacol. 2010;80:1021–32.
19. Yallapu MM, Jaggi M, Chauhan SC. beta-Cyclodextrin-curcumin self-assembly enhances curcumin delivery in prostate cancer cells. Colloids Surf B Biointerfaces. 2010;79:113–25.
20. Higuchi T, Connors KA. Phase solubility techniques. Adv Anal Chem Instrum. 1965;4:117–212.
21. Renner S, Schwab CH, Gasteiger J, Schneider G. Impact of conformational flexibility on three-dimensional similarity searching using correlation vectors. J Chem Inf Model. 2006;46:2324–32.
22. Anderson AM, Mitchell MS, Mohan RS. Isolation of curcumin from turmeric. J Chem Ed. 2000;77:359–60.
23. Shen YL, Ying W, Yang SH, Wu LM. Determinations of the inclusion complex between gossypol and beta-cyclodextrin. Spectrochim Acta A Mol Biomol Spectrosc. 2006;65:169–72.
24. Wu H, Liang H, Yuan Q, Wang T, Yan X. Preparation and Stability investigation of the inclusion complex of sulforaphane with hydroxypropyl-beta-cyclodextrin. Carbohydr Polym. 2010;82:613–7.
25. Song LX, Wang HM, Guo XQ, Bai L. A comparative study on the binding behaviors of beta-cyclodextrin and its two derivatives to four fanlike organic guests. J Org Chem. 2008;73:8305–16.
26. Uner M. Preparation, characterization and physico-chemical properties of solid lipid nanoparticles (SLN) and nanostructured lipid carriers (NLC): their benefits as colloidal drug carrier systems. Pharmazie. 2006;61:375–86.
27. Santander-Ortega MJ, Bastos-Gonzalez D, Ortega-Vinuesa JL, Alonso MJ. Insulin-loaded PLGA nanoparticles for oral administration: an *in vitro* physico-chemical characterization. J Biomed Nanotechnol. 2009;5:45–53.
28. Craparo EF, Cavallaro G, Bondi ML, Mandracchia D, Giammona G. PEGylated Nanoparticles based on a polyaspartamide. preparation, physico-chemical characterization, and intracellular uptake. Biomacromolecules. 2006;7:3083–92.
29. Lemarchand C, Gref R, Lesieur S, Hommel H, Vacher B, Besheer A, *et al.* Physico-chemical characterization of polysaccharide-coated nanoparticles. J Control Release. 2005;108:97–111.
30. Horvath G, Premkumar T, Boztas A, Lee E, Jon S, Geckeler KE. Supramolecular nanoencapsulation as a tool: solubilization of the anticancer drug trans-dichloro(dipyridine)platinum(II) by complexation with beta-cyclodextrin. Mol Pharm. 2008;5:358–63.
31. Yallapu MM, Jaggi M, Chauhan SC. Poly(beta-cyclodextrin)/curcumin self-assembly: a novel approach to improve curcumin delivery and its therapeutic efficacy in prostate cancer cells. Macromol Biosci. 2010;10:1141–51.
32. Komura T, Yamaguchi T, Noda K, Hayashi S. Inclusion complexation of (11-ferrocenylundecyl)trimethylammonium bromide by beta-cyclodextrin and its effects on elctrochemical behavior of the surfactant. Electrochim Acta. 2002;47:3315–25.
33. Kolivoska V, Ga'l M, Hromadova M, Valasek M, Pospisil L. Correlation of the formation constant of ferrocene-cyclodextrin complexes with dielectric properties of the aqueous DMSO solution. J Organomet Chem. 2011;696:1404–8.
34. Srinivasan K, Kayalvizhi K, Sivakumar K, Stalin T. Study of inclusion complex of beta-cyclodextrin and diphenylamine: photophysical and electrochemical behaviors. Spectrochim Acta A Mol Biomol Spectrosc. 2011;79:169–78.
35. Garnero C, Zoppi A, Genovese D, Longhi M. Studies on trimethoprim:hydroxypropyl-beta-cyclodextrin: aggregate and complex formation. Carbohydr Res. 2010;345:2550–6.

36. Inoue Y. NMR studies of the structure and properties of cyclodextrins and their inclusion complexes. Annu Re NMR Spectrosc. 1993;27:59–101.
37. Bernini A, Spiga O, Ciutti A, Scarselli M, Bottoni G, Mascagni P, *et al.* NMR studies of the inclusion complex between beta-cyclodextrin and paroxetine. Eur J Pharm Sci. 2004;22:445–50.
38. Marcolino VA, Zanin GM, Durrant LR, Benassi MT, Matioli G. Interaction of curcumin and bixin with beta-cyclodextrin: complexation methods, stability, and applications in food. J Agric Food Chem. 2011;59:3348–57.
39. Faucci MT, Melani F, Mura P. Computer-aided molecular modeling techniques for predicting the stability of drug-cyclodextrin inclusion complexes in aqueous solutions. Cmeical Physics Letters. 2002;358: 383–90.
40. Jemal A, Bray F, Center MM, Ferlay J, Ward E, Forman D. Global cancer statistics. CA Cancer J Clin. 2011;61:69–90.